Asian Journal of Chemistry; Vol. 33, No. 11 (2021), 2700-2706

ASIAN JOURNAL OF CHEMISTRY

https://doi.org/10.14233/ajchem.2021.23371

Prospect of Poly(2-chloroaniline)-Nanocomposite-Silica as Anode in Li-Ion Coin Cell

G. VANI*, and S. JHANCY MARY

Department of Chemistry, Auxilium College (Autonomous), Vellore-632006, India

*Corresponding author: E-mail: vanichem2005@gmail.com

Received: 16 June 2021; *Accepted*: 8 August 2021; *Published online*: 20 October 2021; AJC-20552

This work evaluates the application of interfacially polymerized poly(2-chloroaniline)-nanocomposite-silica (P2ClAni-SiO_2), a composite material based on substituted conducting polymer, poly(2-chloroaniline) (P2ClAni) in which silica nanoparticles with varying weight percentages act as fillers. The nanocomposites were characterized by FTIR spectroscopy, XRD, TGA and DSC analysis. The electrochemical characterization of P2ClAni and P2ClAni-SiO_2 (10 wt.%) were investigated by cyclic voltammetry, impedance spectroscopy and galvanostatic cycling electrochemical measurements. The cyclic voltammogram studies showed broad redox peaks, which correspond to reversibility in transition of leucoemeraldine to emeraldine form of polyaniline. The charge transfer between electrolyte and electrode was represented in the form of Nyquist plot. The galvanostatic cycling test of P2ClAni and P2ClAni-SiO_2 showed a discharge capacity of 44.3 mAh g^{-1} and 69 mAh g^{-1} for 5 cycles, respectively. P2ClAni-SiO_2 composite shows good electrochemical properties and cycling stability compared to P2ClAni. The chlorosubstituted polyaniline with silica demonstrate to be an anode material in lithium ion batteries.

Keywords: Interfacial polymerization, Nanocomposite, Poly(2-chloroaniline), Nano silica, Coin cell, Anode.

INTRODUCTION

In the past few decades, the progress of conducting polymer with inorganic materials for optics and electronics related applications have gained much attention among researchers [1]. Particularly, the most probable conducting polymer was polyaniline due to its ease of preparation, environmental stability, good electrical conductivity and potential usage in rechargeable batteries, photovoltaic cells, sensors, electromagnetic shielding, gas-separation membranes, light-emitting diodes *etc.* [2-4]. Though its potential applications are very wide, serious problems exist which obstruct its practical use. The major drawback of this polymer is solubility and processability. It can then be replaced by synthesizing derivatives in order to obtain materials with improved solubility and processability, enhanced electrochemical and electronic properties [5-7]. Modified polyaniline can be synthesized by (i) introduction of substituents like -CH_3, -C_2H_5, -halogen and amino groups onto the aromatic rings of the polyaniline chains [8-10] and (ii) copolymerization of aniline and derivatives [11,12].

The halogenated derivatives of polyaniline such as polychloroanilines, polybromoanilines and polyiodoanilines are relatively less investigated. One among the important derivatives of polyaniline is poly(2-chloroaniline) (P2ClAni) and has been studied by few researchers in the recent past. The P2ClAni properties can be fine tuned by a number of ways such as copolymerization, synthesis of blends and composites for applications in the field of hybrid electric devices [13].

Nano-scaled P2ClAni and its effect on oxidant concentration, surfactant type and surfactant concentration were investigated and the results substantiate that the electrical conductivity of doped P2ClAni/SDS50 increased with the monomer: doping ratio of 1:25 possessing the highest electrical conductivity of 10.47 S cm^{-1}, relative to the synthesized P2ClAni without doping [14]. The effect of dodecyl benzene sulphonic acid (DBSA) on the electrical conductivity of P2ClAni and P2ClAni/silk blends has been reported by Linganathan & Samuel [15]. Since P2ClAni-DBSA/Silk has higher dielectric constant than P2ClAni-DBSA and P2ClAni/Silk, it can be used in energy storage devices. Palaniappan [16] studied the effect of temperature on the conductivity and spectral properties of P2ClAni. The methanesulfonic acid doped P2ClAni has been successfully synthesized and shows potential sensing for NH_3 gas [17]. The P2ClAni/SiO_2 nanocomposite was synthesized

and the solubility, thermal stability, electrical conductivity and magnetic properties were investigated by Gok & Sen [18].

The most widely used promising power source for electric vehicles and mobile devices is Li ion battery due to its high energy and power density [19,20]. Graphite and silicon are commonly used anodic materials for Li ion batteries of which graphite showed low specific capacity of 372 mAh g^{-1} and silicon has high theoretical capacity of ~4200 mAh g^{-1} but it has low discharge potential (~0.5 V *vs.* Li/Li^+) [21,22]. Cai *et al.* [23] reported the enhanced cycling stability and rate performance of the nano-silicon/PAni conductive matrix composite and obtained good lithium storage capacity. Encapsulating nano-silicon on PAni matrix showed better reversible capacity of 766.6 mAh g^{-1}, capacity retention of 72% at a current density of 2 Ag^{-1} and are promising Si-based anodic materials for lithium ion batteries as studied by Feng *et al.* [24]. The graphene encapsulated pyrolyzed PAni-grafted Si composites exhibited enhanced cycling stability, rate performance and coulombic efficiency as anodes. The composites deliver a reversible specific capacity of 50 mAh g^{-1} at a charge/discharge rate of 100 A g^{-1} [25].

The mechanism of doping of Li through the interaction with the imine site nitrogen has been proposed for PAni films doped with $LiPF_6$ and $LiBF_4$ which were used as polymer electrodes in lithium secondary batteries [26]. The synthesized $LiNi_{0.8}Co_{0.15}Al_{0.05}O_2$/PAni composite revealed good electrochemical properties at a high discharge rate and the material showed good reversibility for Li insertion in discharge cycles when used as a cathode material [27]. The reduced graphene oxide-SnO_2-PAni composite showed excellent electrochemical performance of high capacity (1017 mAh g^{-1} at 200 mA g^{-1} for the 2nd cycle), superior rate capability (397 mAh g^{-1} at a current density of 10 A g^{-1}) and cyclic stability (1280 mAh g^{-1} after 200 cycles) [28]. The cyclic voltammetry curve showed the peak voltage of 2.49 V while charging and 1.4 V during discharging when P2ClAni-silk was coated as an anodic material [29]. The electrochemical application of P2ClAni based materials in Li ion batteries has not been reported.

The polyaniline derivatives *viz*. P2ClAni and P2ClAni-SiO_2 were interfacially polymerized and characterized by FTIR and XRD spectroscopic techniques. The thermal properties were investigated using TGA and DSC. The electrical performance of the active anodic materials was studied by cyclic voltammetry and galvanostatic cycling test.

EXPERIMENTAL

Poly(2-chloroaniline) (P2ClAni), ammonium persulfate (APS) and hydrochloric acid purchased from Avra, $CHCl_3$ from Isochem were of analytical grade and used as received. The purified grade nano-silica dispersion type A of average particle size of 20 nm was purchased from SRL Pvt. Ltd. India.

Interfacial polymerization of P2ClAni-nanocomposite-SiO_2: The preparation of P2ClAni was done according to interfacial polymerization as reported earlier [28]. In general, interfacial polymerization results in fast polymer chain growth and polymer precipitation at the liquid-liquid interface. This technique involves the combination of two liquid phases namely organic and aqueous phase [29]. In this work, the organic phase was prepared by dissolving 2-chloroaniline in chloroform and the aqueous phase by dissolving ammonium persulfate in HCl. The aqueous solution was carefully poured into the organic solution. By mixing the aqueous and organic reactants slowly, the green P2ClAni was first formed at the interface. The reaction product migrated gradually into the aqueous phase until the whole aqueous phase was filled with homogeneous dark green P2ClAni. The aqueous phase was collected after 24 h of reaction by filtration, the precipitate was washed with deionized water and methanol several times to remove the low molecular weight polymers and oligomers. The dark green coloured material was dried and stored in vials kept in the desiccator. Since interfacial polymerization occurs only at the interface, the secondary growth of polymer was restricted. To prepare nanocomposites, inorganic particles (nano-silica with various wt.%) was mixed in the organic phase. The nano-silica particles have the tendency to assemble at the interface to minimize the surface energy, moving into the interfacial polymerization reaction zone. The polymer nanocomposites are formed in the aqueous phase and the same procedure was followed.

Characterization: FT-IR spectra were obtained using a Thermo Nicolet model in the range 4000-400 cm^{-1}. The XRD patterns were collected using D8 Advance X-ray diffractometer with high-intensity Cu$K\alpha$ (35 mA, 40 kV) radiation and in the 2θ range of 10 to 80 ºC. Perkin-Elmer Thermal Analyzer was used to investigate the thermal stability of the samples at the heating rate of 20 ºC/min from 40 to 800 ºC under nitrogen atmosphere. Electrochemical impedance spectroscopy measurement of the polymer electrolytes was carried out using the electrochemical workstation (CHI Model 608E) over the frequency range from 10 Hz to 0.1 MHz with a symmetrical cell set-up stainless steel (SS) disc/electrolyte film/SS disc for mounting the electrolyte samples.

The electrochemical studies were performed with a CR-2032 coin type cells assembled in an Argon filled glove box. The operating electrode was prepared by mixing the polymer composite with carbon black and polyvinylidene fluoride (PVDF) at a weight ratio of 8:1:1 in 1-methyl-2-pyrrolidone to form slurry. This slurry was layered on a Cu foil, dried and cut into circular discs to use in the cell assembly as anode. Pure Li foil was used as the counter electrode. The electrodes were separated by a glass fiber soaked in 1 M $LiPF_6$ in ethylene carbonate (EC)/dimethyl carbonate (DMC) (1:1 by volume).

Electrochemical impedance measurements were conducted on a CHI660C work station by scanning from 1 MHz to 10 MHz at AC amplitude of 5 mV. Cyclic voltammograms were recorded using Autolab PGSTAT302n for a CR-2032 coin type cells, which formed a three electrode cell. The working electrode (active anode material) was combined with a Li-foil used as reference and counter electrode and a scan rate of 0.1 mV s^{-1} between 0.1-3.0 V *vs.* Li was set.

The galvanostatic charging and discharging were performed using a battery testing system, within the voltage range of 0.1-3.0 V. For the cycling test, the working electrodes were cycled at a charge and discharge current density of 10 μA/cm^2 for P2ClAni and P2ClAni-SiO_2.

RESULTS AND DISCUSSION

FTIR spectra: Fig. 1 shows the FTIR spectra of P2ClAni (a) and P2ClAni-SiO_2 nanocomposites (b) 5wt.% (c) 10 wt.% (d) 20 wt.% (e) 30 wt.%. The main bands observed for P2ClAni are N-H stretching at 3226 cm^{-1}, quinonoid rings at 1564 cm^{-1}, benzenoid rings at 1492 cm^{-1} [30,31] and -CH out of plane bending vibration of 1,2,4-trisubstituted aromatic rings at 896 and 827 cm^{-1}. The peak at 1328 cm^{-1} is due to the aromatic C-N stretching vibration. The peak at 744 cm^{-1} corresponds to the chlorine atoms attached to the phenyl rings. The vibrations around 1089 cm^{-1} are due to an electronic-like band and are indicative of P2ClAni conductivity [32].

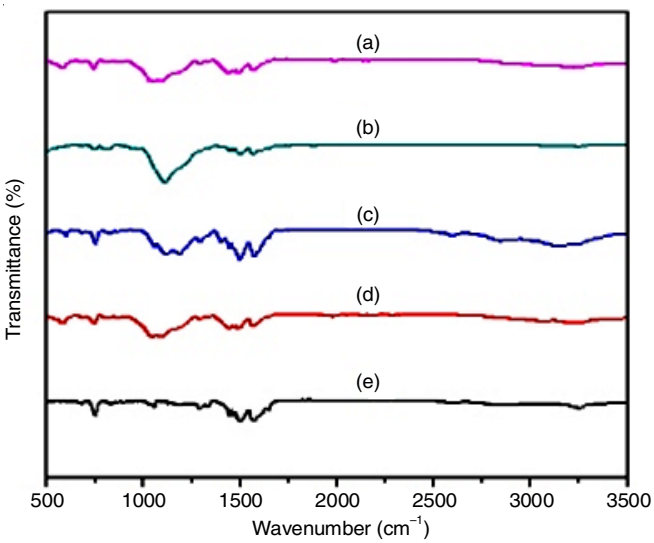

Fig. 1. FTIR spectra of P2ClAni (a) and P2ClAni-SiO_2 nanocomposites (b) 5wt% (c) 10 wt% (d) 20 wt% (e) 30 wt%

In the FTIR spectra of P2ClAni-SiO_2 (5 wt.% silica), shifts in the wavenumbers were observed after the addition of nano-silica. The peaks at 1089, 1328, 1492 and 1564 cm^{-1} were shifted to 1056, 1289, 1499 and 1577 cm^{-1}, respectively, which confirmed the encapsulation of nano-silica into the P2ClAni chains [17]. The peak due to N-H stretching was shifted towards higher wavenumber at 3251 cm^{-1}. The peak observed at 1034 cm^{-1} is related to the Si–O–Si stretching vibration from nano-silica. The vibration around 1056 cm^{-1} corresponds to an electronic-like band and indicates the charged structure. The characteristic stretching frequencies were shifted towards the lower and higher frequency sides in the composite when compared to the polymer. All these peaks clearly revealed the emeraldine salt form and the interaction between nano-silica and P2ClAni. The same shifts were also observed in the polymer composites with 10, 20 and 30% nano-silica, which confirm the formation of P2ClAni-SiO_2. The characteristic assignments are tabulated in Table-1.

XRD: Fig. 2 shows the XRD patterns of P2ClAni and P2ClAni-SiO_2 (10 wt.%). The crystalline nature of P2ClAni and P2ClAni-SiO_2 composite was observed. The main diffraction peak of P2ClAni synthesized by interfacial method at 2θ = 26.5º represents the presence of P2ClAni [33]. Similarly, the spectrum of the silica composite exposed a diffraction peak, revealing the semicrystalline nature of the nanocomposite. The decrease in the intensity may be due to nano-silica dispersion in polymer matrix and interface interaction with P2ClAni. As a result, the addition of silica nanoparticles may hinder the degree of crystallization and attains lower crystallinity.

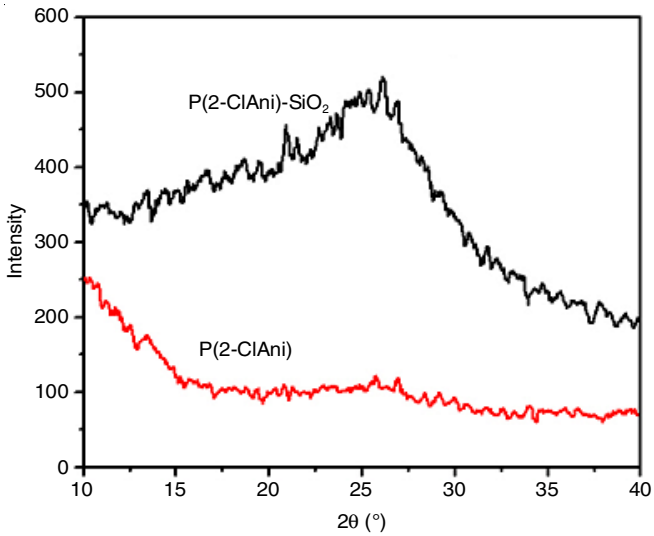

Fig. 2. XRD patterns of P2ClAni and P2ClAni-SiO_2 (10 wt%)

Thermal studies: Figs. 3 and 4 show the TGA of P2ClAni and P2ClAni-SiO_2 nanocomposite (10 wt.%), respectively. The polymer begins to react with oxygen in air at low temperature and loses the majority of its mass from 400-800 ºC. The composite loses the majority of its mass from 350-800 ºC indicating the oxidation and decomposition. The thermal stability was also studied by calculating the integral procedural decomposition temperature (IPDT) and oxidation index (OI) values according to the procedure developed by Doyle [34]. From the decomposition temperature IPDT and OI values, the presence

TABLE-1
FTIR ASSIGNMENTS OF P2ClAni AND P2ClAni-SiO_2 NANOCOMPOSITES

Peak assignments (cm^{-1})	P2ClAni	P2ClAni-SiO_2 (5 wt%)	P2ClAni-SiO_2 (10 wt%)	P2ClAni-SiO_2 (20 wt%)	P2ClAni-SiO_2 (30 wt%)
N-H stretching	3226	3251	3225	3129	3246
-C=C- stretching of benzenoid rings	1492	1499	1493	1499	1499
-C=C- stretching of quinonoid rings	1564	1577	1569	1577	1568
C-Cl stretching	744	754	745	754	748
Electrical conductivity band	1089	1188	1187	1115	1111
Asymmetric stretching of Si-O-Si	–	1034	1050	1057	1111
Symmetric stretching of Si-O-Si	–	829	820	827	810
Asymmetric Bending of Si-O	–	480	434	479	474

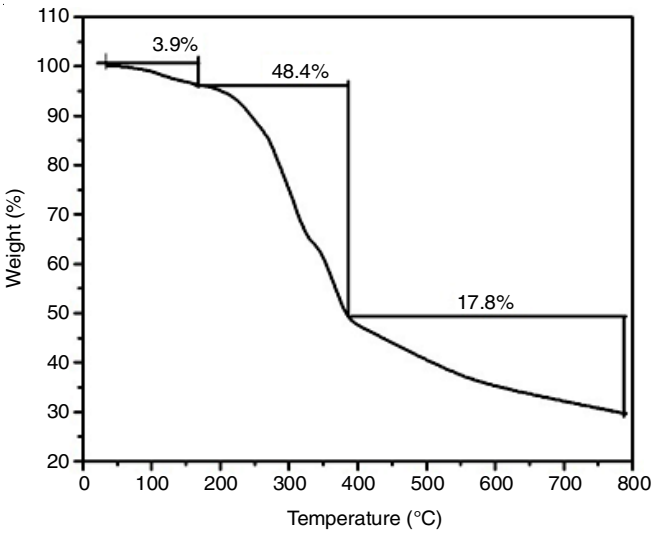

Fig. 3. TGA curve of P2ClAni

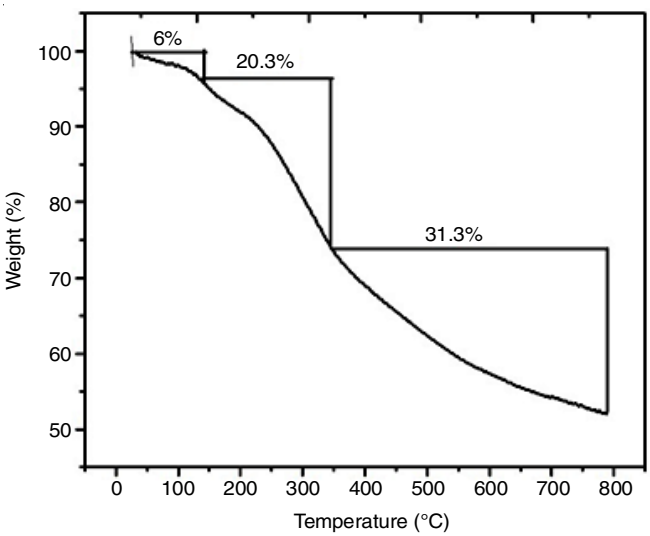

Fig. 4. TGA curve of P2ClAni-SiO_2 (10 wt%)

of nano-silica enhanced the thermal stability of polymer composite as shown in Table-2.

TABLE-2
IPDT AND OI VALUES OF P2CLANI AND P2CLANI-SiO_2 (10 wt%)

Polymer	IPDT (°C)	OI value
P2ClAni	352	0.0469
P2ClAni-SiO_2 (10 wt%)	472	0.0755

The glass transition temperatures of P2ClAni and P2ClAni-SiO_2 using DSC under inert atmosphere at a scan rate of 20 ºC/min are shown in Figs. 5 and 6, respectively. The DSC curve of P2ClAni-SiO_2 shows a glass transition temperature of 156 ºC with the specific heat capacity of 69.14 J/g. The decomposition temperature of P2ClAni was 520 ºC, while of P2ClAni-SiO_2 was 650 ºC. The P2ClAni-SiO_2 was thermally more stable than P2ClAni.

Electrochemical measurements: Nyquist plots of P2ClAni and P2ClAni-SiO_2 (10 wt.% of SiO_2) are shown in Fig. 7. Based

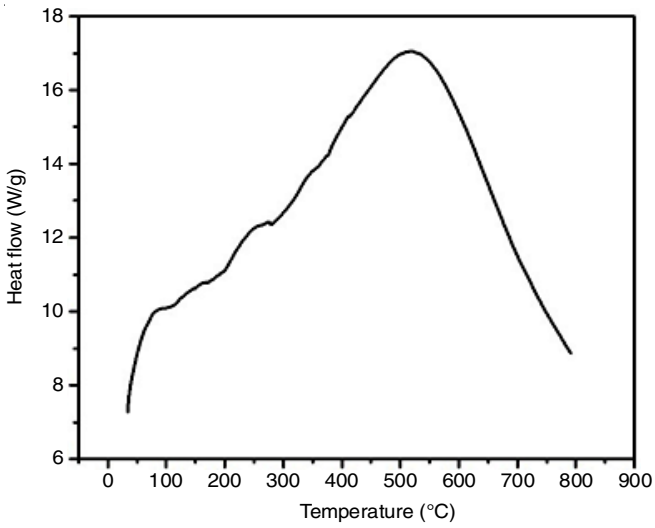

Fig. 5. DSC curve of P2ClAni

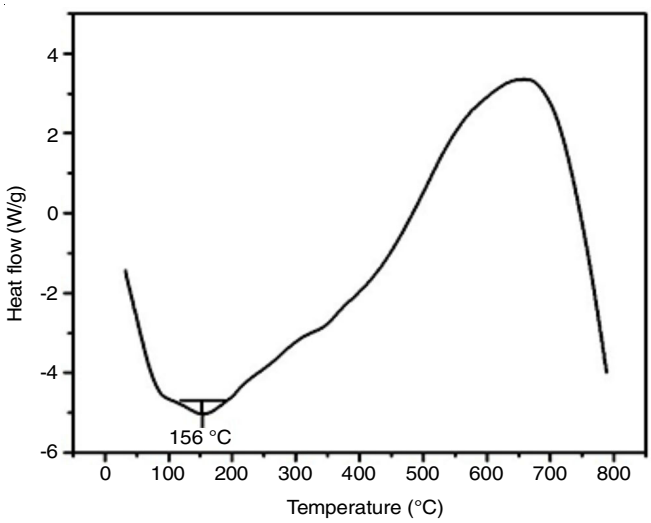

Fig. 6. DSC curve of P2ClAni-SiO_2 (10 wt%)

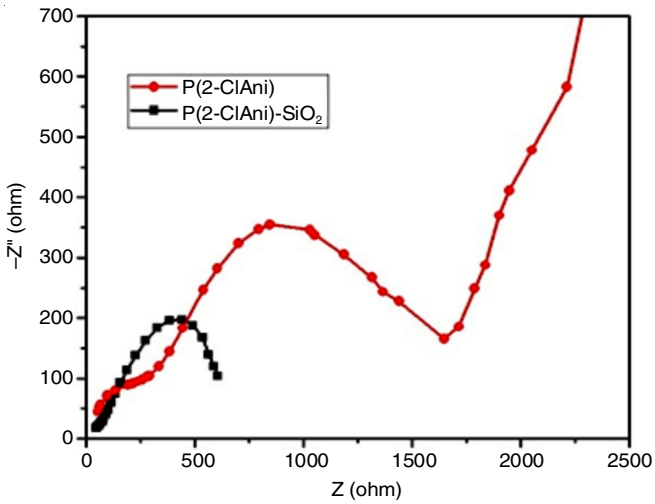

Fig. 7. Nyquist plots of P2ClAni and P2ClAni-SiO_2 (10 wt% of SiO_2)

on the Nyquist plot of P2ClAni, the slope at the low frequency was related to Li-ion diffusion [35], which expresses the ionic diffusion behaviour and exhibits a 45º slope.

The charge transfer resistance R_{ct} of P2ClAni and SiO_2 nanocomposites were found to be 1600 and 600 ohm. The lower charge transfer resistance in the P2ClAni-SiO_2 nanocomposite associates with the higher conductivity and the large surface area of the composite. It suggests that the impedance responses in the low-frequency region indicate a Faradaic process of the bulk redox transitions of the polymer P2ClAni. The decrease in the specific capacity was attributed to an increase in charge transfer resistance and a decrease in the diffusion coefficient as measured by electrochemical impedance spectroscopy. From the above discussion, it is well proved that the P2ClAni and its nanocomposite material have electrochemical storage capability.

The higher percentages of nano-silica (20, 30 wt.%) were polymerized to evaluate the improvement behaviour in the conductivity of the composites due to the increase in the weight percentage of silica. The electrical conductivity of P2ClAni and P2ClAni-SiO_2 nanocomposites (with various wt.%) was found to be in the range of 10^{-3} S cm^{-1} as represented in Table-3. The conductivity of the P2ClAni was in close proximity to the value as observed by Benykhlef *et al*. [36]. The result shows that nano-silica composites have better electrical conductivity than pure substituted polyanilines. This enhanced conductivity is due to incorporation of nano-silica particles into the polymer matrix and this may improve the potential application of the polymer nanocomposites.

Fig. 8 shows the cyclic voltammetry of P2ClAni electrode at a scan rate at 0.1 mV s^{-1} and a voltage range of 0.1 and 3.0 V. It is clear that the main redox peaks (broad in appearance) obtained, which shows anodic at 1.5 V indicating oxidation and cathodic peak at 1.25 V for reduction. The redox peak corresponds to the transition of the leucoemeraldine to emeraldine on the forward scan and on the backward scan switching back to leucoemeraldine.

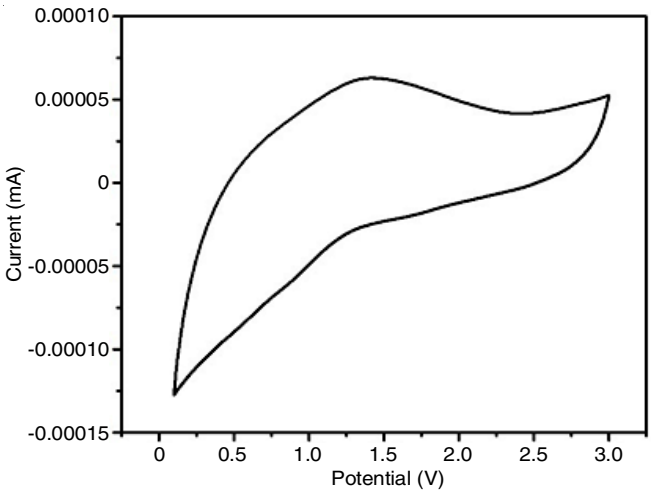

Fig. 8. Cyclic Voltammetry of P2ClAni electrode between 0.1 and 3.0 V at a scan rate of 0.1 mV s^{-1}

The cyclic voltammetry of P2ClAni-SiO_2 electrode is shown in Fig. 9 with the voltage of 0.1-0.3 V. It apparently depicts that the incorporation of SiO_2 induces a slight variation in path with the reversibility of the electrochemical process, by showing the reduction peak at 1.4 V attributed to the formation of Li-Si alloy phases and anodic peak at 0.5 V to 1.2 V due to the reverse de-alloying of Li-Si. This is due to the possibility of slow diffusion of lithium ion transfer during redox system or modification of the structure of P2ClAni by the incorporation of SiO_2 nanoparticle during polymer growth [37].

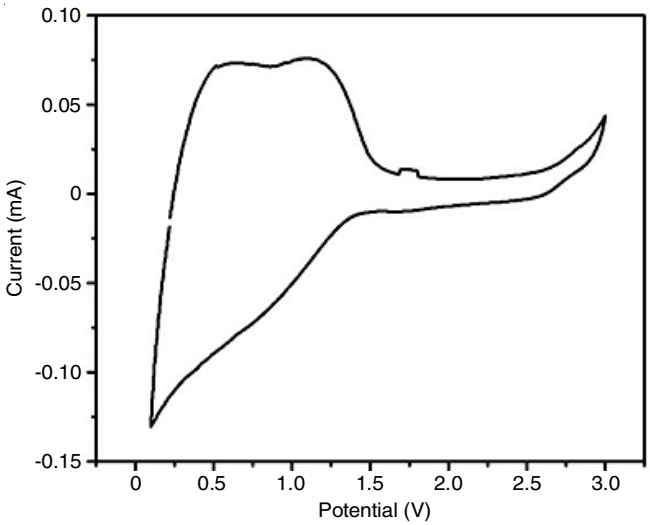

Fig. 9. Cyclic voltammetry of P2ClAni-SiO_2 electrode between 0.1 and 3.0 V at a scan rate of 0.1 mV s^{-1}

Fig. 10 shows the charging and discharging curve of P2ClAni/$LiPF_6$ (EC+DMC)/Li coin cell for first cycle at current density of 10 μA/cm^2 with a voltage window of 0.2-3 V. Fig. 12 shows the charging and discharging curve of P2ClAni-SiO_2/$LiPF_6$ (EC+DMC)/Li coin cell for first cycle at current density of 10 μA/cm^2 with a voltage window of 0.2-3 V. Figs. 11 and 13 show the galvanostatic cycling behaviour of P2ClAni and P2ClAni-SiO_2, respectively.

Coin cell with P2ClAni based electrode delivered an initial discharge capacity of 44.3 mAh/g and then rapidly decreased to 39.5 mAh/g at the fifth cycle. The discharging capacity of P2ClAni-SiO_2 based electrode was found to be 69 mAh/g and at end of the fifth cycle it was 30 mAh/g. This decrease in specific capacity could be ascribed to the large change in volume due to structural deterioration or may be increase in electrode polarization during cycling.

The practical discharge capacity of P2ClAni-SiO_2 (69 mAh g^{-1}) was 48% of the theoretical value and the practical discharge capacity of P2ClAni (44.3 mAh g^{-1}) was 21% of the theoretical value [38]. The cell based on nano-silica composite electrode shows good performance in cycling stability and higher discharge capacity than P2ClAni.

TABLE-3
ELECTRICAL CONDUCTIVITY VALUES OF P2ClAni AND P2ClAni-SiO_2 COMPOSITES

Polymer samples	P2ClAni	P2ClAni (5 wt%)	P2ClAni (10 wt%)	P2ClAni-SiO_2 (15 wt%)	P2ClAni-SiO_2 (20 wt%)
Conductivity (S cm^{-1})	0.14×10^{-3}	2.5×10^{-3}	0.17×10^{-3}	3.25×10^{-3}	3.67×10^{-3}

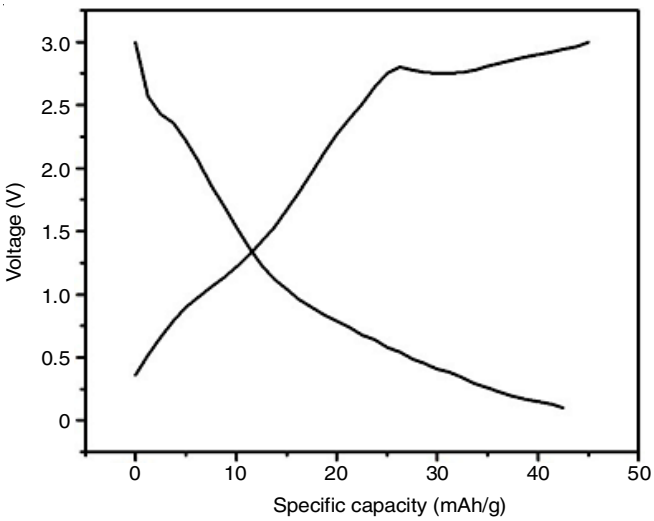

Fig. 10. Charging and discharging curve of P2ClAni/$LiPF_6$ (EC+DMC)/Li coin cell for first cycle at current density of 10 μA/cm^2 with a voltage window of 0.2-3 V

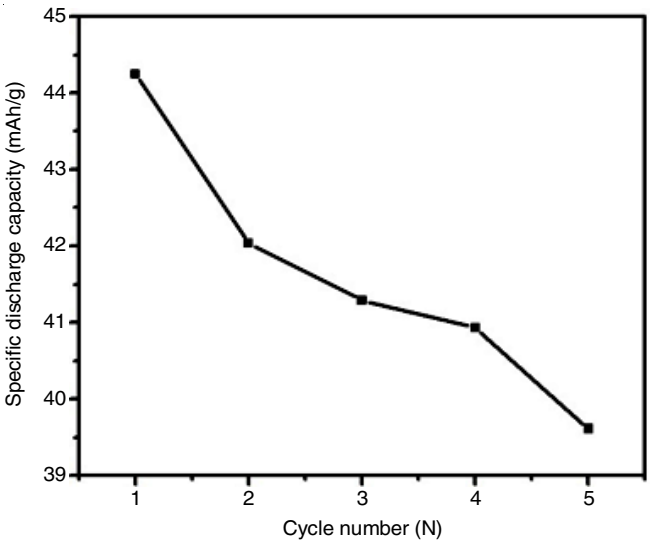

Fig. 11. Galvanostatic cycling behaviour of P2ClAni

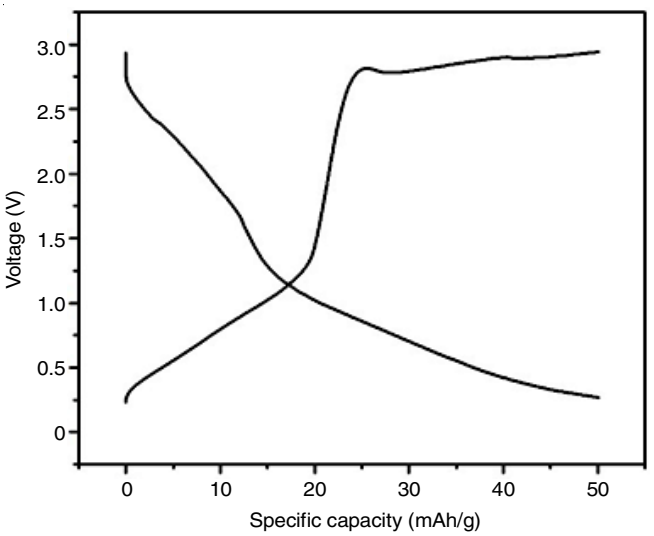

Fig. 12. Charging and discharging curve of P2ClAni-SiO_2/$LiPF_6$ (EC+DMC)/Li coin cell for first cycle at current density of 10 μA/cm^2 with a voltage window of 0.2-3 V

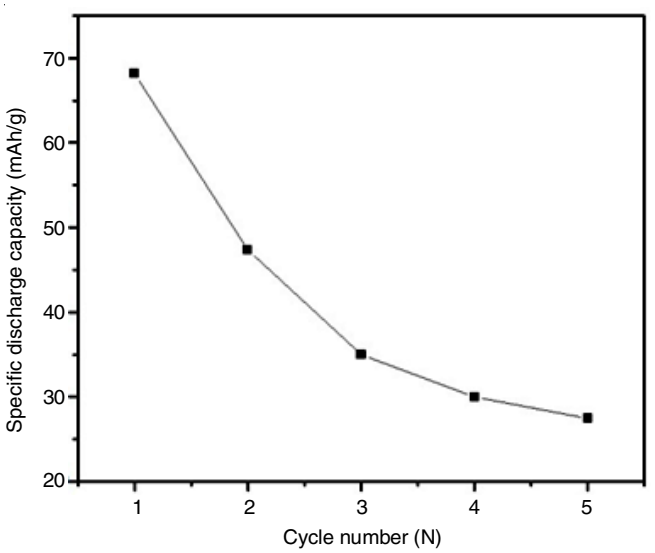

Fig. 13. Galvanostatic cycling behaviour of P2ClAni-SiO_2

Conclusion

Herein, P2ClAni-SiO_2 nanocomposites were synthesized in conducting emeraldine forms by interfacial polymerization. The spectral results indicate that there was interaction between nano-silica and P2ClAni and the nanocomposites exist with reduced crystalline nature. The electrical conductivities of P2ClAni and P2ClAni-SiO_2 (10 wt.%) were 1.4×10^{-4} S cm^{-1} and 1.7×10^{-4} S cm^{-1}, respectively. Thermogravimetric analysis results confirmed that the P2ClAni-SiO_2 (10 wt.%) showed good thermal stability and higher IPDT and OI values relative to P2ClAni. The cyclic voltammograms showed broad redox peaks indicating reversible Li ion intercalation. The migration of Li ion through the interface, is indicated by high frequency semicircle. The galvanostatic charge/discharge profile showed moderate discharge capacity for P2ClAni of 44.3 mAh g^{-1} at 10 μA/cm^2 and P2ClAni-SiO_2 composite of 69 mAh g^{-1} at 10 μA/cm^2 in 5 cycles. From the above discussion, it is suggested that P2ClAni-SiO_2 can be considered as a good matrix anodic material for lithium ion batteries. However, the detailed studies on synthesis and fabrication of P2ClAni and its nano-silica composite are still needed to meet the requirements for electrode in lithium ion battery applications.

CONFLICT OF INTEREST

The authors declare that there is no conflict of interests regarding the publication of this article.

REFERENCES

1. K. Namsheer and C.S. Rout, *RSC Adv.*, **11**, 5659 (2021); https://doi.org/10.1039/D0RA07800J
2. J.X. Huang and R.B. Kaner, *J. Am. Chem. Soc.*, **126**, 851 (2004); https://doi.org/10.1021/ja0371754
3. N.-R. Chiou and A.J. Epstein, *Adv. Mater.*, **17**, 1679 (2005); https://doi.org/10.1002/adma.200401000
4. P. Sengodu and A.D. Deshmukh, *RSC Adv.*, **5**, 42109 (2015); https://doi.org/10.1039/C4RA17254J
5. R. Balint, N.J. Cassidy and S.H. Cartmell, *Acta Biomater.*, **10**, 2341 (2014); https://doi.org/10.1016/j.actbio.2014.02.015

6. U.A. Sevil, E. Coskun and O. Güven, *Radiat. Phys. Chem.*, **94**, 45 (2014); https://doi.org/10.1016/j.radphyschem.2013.07.029
7. Z. Zhang, Z. Wei and M. Wan, *Macromolecules*, **35**, 5937 (2002); https://doi.org/10.1021/ma020199v
8. G. Ravi Kumar, J. Vivekanandan, A. Mahudeswaran and P.S. Vijayanand, *Iran. Polym. J.*, **22**, 923 (2013); https://doi.org/10.1007/s13726-013-0191-x
9. P.S. Vijayanand, J. Vivekanandan, A. Mahudeswaran, G. Ravi Kumar and R. Anandarasu, *Des. Monomers Polym.*, **18**, 12 (2015); https://doi.org/10.1080/15685551.2014.947548
10. X.G. Li, M.R. Huang, W. Duan and Y.L. Yang, *Chem. Rev.*, **102**, 2925 (2002); https://doi.org/10.1021/cr010423z
11. W. Shenglong, W. Fosong and G. Xiaohui, *Synth. Met.*, **16**, 99 (1986); https://doi.org/10.1016/0379-6779(86)90158-X
12. S. Palaniappan, *Polym. Int.*, **49**, 659 (2000); https://doi.org/10.1002/1097-0126(200007)49:7<659::AID-PI427>3.0.CO;2-L
13. A. Andriianova, Y.N. Biglova and A.G. Mustafin, *RSC Adv.*, **10**, 4768 (2020); https://doi.org/10.1039/C9RA08644G
14. W. Kongkaew, W. Sangwan, W. Prissanaroon-Ouajai and A. Sirivat, *Chem. Pap.*, **72**, 1007 (2018); https://doi.org/10.1007/s11696-017-0343-0
15. P. Linganathan and J.M. Samuel, *Am. J. Polym. Sci.*, **4**, 107 (2014).
16. S. Palaniappan, *Polym. Adv. Technol.*, **5**, 263 (1994); https://doi.org/10.1002/pat.1994.220050504
17. S.S. Pandule, S.U. Shisodia, M.R. Patil, V.V. Chabukswar and R.P. Pawar, *J. Macromol. Sci. A Pure Appl. Chem.*, **53**, 768 (2016); https://doi.org/10.1080/10601325.2016.1237815
18. A. Gök and S. Sen, *J. Appl. Polym. Sci.*, **102**, 935 (2006); https://doi.org/10.1002/app.24266
19. M. Armand and J.M. Tarascon, *Nature*, **451**, 652 (2008); https://doi.org/10.1038/451652a
20. Y.-G. Guo, J.-S. Hu and L.J. Wan, *Adv. Mater.*, **20**, 2878 (2008); https://doi.org/10.1002/adma.200800627
21. Y.S. Hu, R. Demir-Cakan, M.M. Titirici, J.O. Müller, R. Schlögl, M. Antonietti and J. Maier, *Angew. Chem. Int. Ed.*, **47**, 1645 (2008); https://doi.org/10.1002/anie.200704287
22. A. Magasinski, B. Zdyrko, I. Kovalenko, B. Hertzberg, R. Burtovyy, C.F. Huebner, T.F. Fuller, I. Luzinov and G. Yushin, *ACS Appl. Mater. Interfaces*, **2**, 3004 (2010); https://doi.org/10.1021/am100871y
23. J.-J. Cai, P.-J. Zuo, X.-Q. Cheng, Y.-H. Xu and G.-P. Yin, *Electrochem. Commun.*, **12**, 1572 (2010); https://doi.org/10.1016/j.elecom.2010.08.036
24. M. Feng, J. Tian, H. Xie, Y. Kang and Z. Shan, *J. Solid State Electrochem.*, **19**, 1773 (2015); https://doi.org/10.1007/s10008-015-2807-x
25. Z.-F. Li, H. Zhang, Q. Liu, Y. Liu, L. Stanciu and J. Xie, *ACS Appl. Mater. Interfaces*, **6**, 5996 (2014); https://doi.org/10.1021/am501239r
26. K.S. Ryu, K.M. Kim, S.G. Kang, G.J. Lee, J. Joo and S.H. Chang, *Synth. Met.*, **110**, 213 (2000); https://doi.org/10.1016/S0379-6779(99)00288-X
27. Y.-M. Chung and K.-S. Ryu, *Bull. Korean Chem. Soc.*, **30**, 1733 (2009); https://doi.org/10.5012/bkcs.2009.30.8.1733
28. H. Liu, B.H. Liu and Z.P. Li, *Solid State Ion.*, **294**, 6 (2016); https://doi.org/10.1016/j.ssi.2016.06.008
29. A. Abdolahi, E. Hamzah, Z. Ibrahim and S. Hashim, *Materials*, **5**, 1487 (2012); https://doi.org/10.3390/ma5081487
30. S.X. Xing, H.W. Zheng and G.K. Zhao, *Synth. Met.*, **158**, 59 (2008); https://doi.org/10.1016/j.synthmet.2007.12.004
31. T.Q. Wang, W.B. Zhong, X.T. Ning, Y.X. Wang and W.T. Yang, *J. Colloid Interface Sci.*, **334**, 108 (2009); https://doi.org/10.1016/j.jcis.2009.03.013
32. M.E. Plonska-Brzezinska, J. Mazurczyk, B. Palys, J. Breczko, A. Lapinski, A.T. Dubis and L. Echegoyen, *Chem. Eur. J.*, **18**, 2600 (2012); https://doi.org/10.1002/chem.201102175
33. A. Gök, H.K. Can, B. Sari and M. Talu, *Mater. Lett.*, **59**, 80 (2005); https://doi.org/10.1016/j.matlet.2004.09.021
34. C.D. Doyle, *Anal. Chem.*, **33**, 77 (1961); https://doi.org/10.1021/ac60169a022
35. P. Vyroubal and T. Kazda, *J. Energy Storage*, **15**, 23 (2018); https://doi.org/10.1016/j.est.2017.10.019
36. S. Benykhlef, A. Bekhoukh, R. Berenguer, A. Benyoucef and E. Morallon, *Colloid Polym. Sci.*, **294**, 1877 (2016); https://doi.org/10.1007/s00396-016-3955-y
37. S. Abaci, B. Nessark and F. Riahi, *Ionics*, **20**, 1693 (2014); https://doi.org/10.1007/s11581-014-1129-9
38. S.B. Sertkol, D. Sinirlioglu, B. Esat and A.E. Muftuoglu, *J. Polym. Res.*, **22**, 136 (2015); https://doi.org/10.1007/s10965-015-0777-4